Effective Model and Magnetic Properties of the Resistive Electron Quadrupling State

Julien Garaud [1,2,*] and Egor Babaev [3,†]

[1]*Institut Denis Poisson CNRS-UMR 7013, Université de Tours, 37200 Tours, France*
[2]*Nordita, Stockholm University, Roslagstullsbacken 23, SE-106 91 Stockholm, Sweden*
[3]*Department of Physics, KTH Royal Institute of Technology, SE-106 91 Stockholm, Sweden*

(Received 14 January 2022; revised 9 May 2022; accepted 30 June 2022; published 16 August 2022)

Recent experiments [Grinenko *et al.* Nat. Phys. **17**, 1254 (2021)] reported the observation of a condensate of four-fermion composites. This is a resistive state that spontaneously breaks the time-reversal symmetry, leading to unconventional magnetic properties, detected in muon spin rotation experiments and by the appearance of a spontaneous Nernst effect. In this Letter, we derive an effective model for the four-fermion order parameter that describes the observed spontaneous magnetic fields in this state. We show that this model, which is alike to the Faddeev-Skyrme model can host skyrmions: magnetic-flux-carrying topological excitations.

DOI: 10.1103/PhysRevLett.129.087602

Recent experiments [1] reported the observation of a fermion quadrupling state in the multiband material: hole-doped $Ba_{1-x}K_xFe_2As_2$. This resistive state, coined quartic bosonic metal, is a condensate with an anticorrelated flow of pairs of Cooper pairs belonging to different bands. In contrast to superconductors, which break the U(1) gauge symmetry, this state spontaneously breaks the two-fold ($\mathbb{Z}_2$) time-reversal symmetry. This raises the question of the properties of such states.

An effective model can describe the properties of condensates at large length scales. For a pair condensate, the effective model is the celebrated Ginzburg-Landau theory which has been extensively studied since the second half of the last century. The question of effective models describing the fermion quadruplet quartic metal is more subtle. In this Letter, we derive an effective long-wavelength model for the resistive quartic state reported in $Ba_{1-x}K_xFe_2As_2$. Based on this, we report the key properties of that state: Namely its magnetic properties and the nature of the topological excitations it supports.

At low temperatures, the compound is a superconductor characterized by Cooper pair condensates Δ_a, forming in the different bands labeled by a. Importantly this superconductor breaks the time-reversal symmetry [2,3], so that the total symmetry broken by the low-temperature state is $U(1)\times\mathbb{Z}_2$. The analysis of the magnitude and polarization of spontaneous magnetic fields [3–5] indicates a spin-singlet superconducting state that breaks the time-reversal symmetry. It is the so-called $s+is$ state which has two energetically equivalent locking of the relative phase $\theta_b-\theta_a$ between the superconducting gaps in different components $\Delta_{a,b}$.

The mechanism responsible for the appearance of the quartic metal is the following: The standard assumption of the Bardeen-Cooper-Schrieffer theory is a mean-field approximation for the fields quadratic in fermions: This assumption eliminates, by construction, the possibility for fermion quadrupling. The resulting theory yields the phase diagram of such a superconductor, which is typically a dome of the $s+is$ state between two different superconducting states [6–10]. It was pointed out in [11,12], that relaxing the mean-field approximation in a multicomponent fermion pairing theory results in a phase diagram with the appearance of fermion quadrupling condensates. The large-scale Monte Carlo calculations of $U(1)\times\mathbb{Z}_2$ states demonstrated that the discrete $\mathbb{Z}_2$ transition can exceed the superconducting U(1) transition: $T_c<T_c^{\mathbb{Z}_2}$ [13–15].

The spontaneous breakdown of the time-reversal symmetry in the resistive state of $Ba_{1-x}K_xFe_2As_2$, at the doping level $x\approx 0.8$ [1] dictates that the averages of the pairing order parameters Δ_a are zero, but that there exists a nonzero order parameter which is fourth order in the fermionic fields. The quadrupling order parameter is proportional to the product of pairing order parameters in different bands $\Delta_a^*\Delta_b$. Such an order parameter implies an anticorrelation in the flows of the components a and b. Crucially, although these types of counterflows do not represent superconductivity, they are generally coupled to the magnetic field when the densities of the counterflowing charged components are unequal. An effective model should account for this coupling, and should be different from the Ginzburg-Landau model of a Meissner state.

Below we derive such an *effective* theory, based on the mean-field approximation for the four-fermion order parameter. We demonstrate that, in an inhomogeneous sample, the model supports spontaneous magnetic fields, consistently with the experimental results [1]. It also predicts the existence of topological excitations carrying a quantized magnetic flux, in the form of skyrmions.

We derive our effective model for a state with composite order from a generic model of a superconductor with a two-component order parameter Ψ, with $\Psi^\dagger \coloneqq (\psi_1^*, \psi_2^*)$. The detailed derivation from the microscopic theory can be found in the Supplemental Material [16]. The generic Ginzburg-Landau free-energy density for a two-component superconductor reads as

$$\mathcal{F}(\Psi, \boldsymbol{A}) = \frac{\boldsymbol{B}^2}{2} + \frac{k_{ab,ij}}{2}(D_i\psi_a)^* D_j\psi_b + V(\Psi^\dagger, \Psi), \quad (1)$$

where $V(\Psi^\dagger, \Psi)$ is the potential energy term. The repeated indices are implicitly summed over, and the indices i, j denote the spatial coordinates while a, b label the different components. The individual condensates are coupled to the vector potential $\boldsymbol{A}$, of the magnetic field $\boldsymbol{B} = \boldsymbol{\nabla} \times \boldsymbol{A}$, via the gauge derivative $\boldsymbol{D} = \boldsymbol{\nabla} + ie\boldsymbol{A}$ in the kinetic term. In this Letter, we focus on two-component models that break multiple symmetries. The symmetry breaking is encoded in the potential term $V(\Psi^\dagger, \Psi)$ which explicitly reduces the global SU(2) symmetry of a doublet of complex order parameters down to a smaller symmetry group. For example, the SU(2) symmetry is broken down to $\mathrm{U}(1) \times \mathbb{Z}_2$, for a superconductor that breaks time-reversal symmetry such as $s + is$, $s + id$, $d + ig$, $p + ip$, or down to $\mathrm{U}(1) \times \mathbb{Z}_3$ symmetry as was suggested for some nematic superconductors [25]. The composite order of interest arises if the fluctuations-driven restoration of the local gauge symmetry occurs without restoring the other broken symmetries. The existence of a composite order was demonstrated in systems featuring $\mathrm{U}(1) \times \mathrm{U}(1)$ [11,12] and SU(2) [26,27] symmetries, and from these calculations it follows that composite order also exists for $\mathrm{U}(1) \times \mathbb{Z}_n$ symmetries. While most of our results qualitatively apply to all of the above mentioned pairing mechanisms, we focus below on the case of the broken time-reversal symmetry $\mathrm{U}(1) \times \mathbb{Z}_2$, and in particular on the $s + is$ state, motivated by the experiment on $\mathrm{Ba}_{1-x}\mathrm{K}_x\mathrm{Fe}_2\mathrm{As}_2$ [1]. Other related states with composite order were discussed in [28–37].

At the microscopic level, the minimal model features three distinct superconducting gaps $\Delta_{1,2,3}$ in three different bands, and the pairing that leads to the time-reversal symmetry breaking states is dominated by the competition between different interband repulsion channels [6,8,10]. In the case of an interband-dominated repulsive pairing, only two fields $\psi_{1,2}$ appear in the effective Ginzburg-Landau model for the superconducting state, see e.g., Refs. [8,38,39]. When starting from the microscopic three-band model, the relevant two-component Ginzburg-Landau theory features mixed-gradient terms, which can be eliminated by a linear transformation to new fields, see e.g., Refs. [39,40] and the Supplemental Material [16]. The resulting Ginzburg-Landau theory is characterized by the free-energy $F/F_0 = \int \mathcal{F}$ whose density reads as

$$\mathcal{F}(\Psi, \boldsymbol{A}) = \frac{\boldsymbol{B}^2}{2} + \frac{1}{2}|\boldsymbol{D}\Psi|^2 + V(\Psi^\dagger, \Psi). \quad (2)$$

To account for the four-fermion state, the Ginzburg-Landau theory (2) is first mapped onto a model that couples the supercurrent $\boldsymbol{J} = e\mathrm{Im}(\Psi^\dagger \boldsymbol{D}\Psi)$ to a real three-vector $\boldsymbol{m}$. It is defined as the projection of the superconducting degrees of freedom Ψ onto spin-1/2 Pauli matrices $\boldsymbol{\sigma}$: $\boldsymbol{m} = \Psi^\dagger \boldsymbol{\sigma} \Psi$; hence this is an order parameter which is fourth order in the fermionic fields. This order parameter depends on the relative phase between the original complex fields, and does not depend on the superconducting degree of freedom: the phase sum. The norm of $\boldsymbol{m}$ is related to the total density squared $\|\boldsymbol{m}\| \equiv \varrho^2 = \Psi^\dagger \Psi$. In terms of $\boldsymbol{J}$ and $\boldsymbol{m}$, the free energy reads as [16]

$$\mathcal{F} = \frac{1}{2}\left[\epsilon_{kij}\left\{\nabla_i\left(\frac{\boldsymbol{J}_j}{e^2\varrho^2}\right) - \frac{1}{4e\varrho^6}\boldsymbol{m}\cdot\partial_i\boldsymbol{m}\times\partial_j\boldsymbol{m}\right\}\right]^2 + \frac{\boldsymbol{J}^2}{2e^2\varrho^2} + \frac{1}{8\varrho^2}(\boldsymbol{\nabla}\boldsymbol{m})^2 + V(\boldsymbol{m}), \quad (3)$$

where ϵ is the rank-3 Levi-Civita symbol. The term in the square brackets in (3) is the magnetic field expressed through gradients of the matter fields. The first term there is the contribution of the Meissner current $\boldsymbol{J}$ to the magnetic field, while the second term accounts for the interband counterflow [41,42]:

$$\boldsymbol{B} = \boldsymbol{\nabla} \times \left(\frac{\boldsymbol{J}}{e^2\varrho^2}\right) - \frac{\epsilon_{abc}}{4e\varrho^6} m_a \boldsymbol{\nabla} m_b \times \boldsymbol{\nabla} m_c. \quad (4)$$

The second term is particularly important: It is related to the counterflow of two components, since it has a form of gradients of the composite field $\psi_a^*\psi_b$, i.e., it depends on gradients of the relative phase between components. A counterflow of two identical charged components results in no charge transfer and hence does not couple to the magnetic field. However, if the densities of the components are locally imbalanced, the charge transport occurs. Thus the coupling to the magnetic field involves a dependence of the relative density gradients.

Next, the low-temperature model (3), which microscopic derivation is given in the Supplemental Material [16], is used to obtain an effective model of the fermion quadrupling phase. The fermion quadrupling phase identified in [1,13,14] is resistive. This is caused by the disorder of the superconducting phase due to the proliferation of topological defects. The effective model of the resulting fermion quadrupling state is obtained by removing the superconducting degrees of freedom from (3). Indeed, as demonstrated in Monte Carlo calculations, their prefactors are renormalized to zero [1,13,14,26,27,30,43,44,45]. It follows that the Meissner current vanishes ($\boldsymbol{J} = 0$), while the currents associated with gradients of the fermion quadrupling order parameter $\boldsymbol{m}$ do not. Assuming that the critical temperatures of the $\mathbb{Z}_2$ and U(1) transitions are well separated, the free energy of the fermion quadrupling state can be written as

$$\mathcal{F}(\boldsymbol{m}) = \frac{(\boldsymbol{m}\cdot\partial_i\boldsymbol{m}\times\partial_j\boldsymbol{m})^2}{16e^2\|\boldsymbol{m}\|^6} + \frac{(\boldsymbol{\nabla}\boldsymbol{m})^2}{8\|\boldsymbol{m}\|} + V(\boldsymbol{m}), \quad (5a)$$

$$\text{where } V(\boldsymbol{m}) = \sum_{a=0,x,y,z} \alpha_a^{\boldsymbol{m}} m_a + \frac{1}{2}\sum_{a,b=0,x,y,z} \beta_{ab}^{\boldsymbol{m}} m_a m_b. \quad (5b)$$

Here the component m_0 stands for the magnitude of $\boldsymbol{m}$, $m_0 \coloneqq \|\boldsymbol{m}\|$ (see details of the microscopic expressions for the coefficients in [16]). The first term in (5) has to be retained because it depends only on the relative phases and densities of the original superconducting fields. Hence it cannot vanish at superconducting phase transition, when $T_c < T_c^{\mathbb{Z}_2}$ [46]. The fermion quadrupling phase reported in [1] breaks the time-reversal symmetry. Hence the potential term (5b) breaks the symmetry associated with the vector $\boldsymbol{m}$ down to $\mathbb{Z}_2$. In the original Ginzburg-Landau model (2), the time-reversal operation is the complex conjugation of the superconducting condensates Ψ. Correspondingly, for the soft modulus vector it is a reflection of $\boldsymbol{m}$ on the xz plane of the target space:

$$\mathcal{T}(\Psi) = \Psi^* \Leftrightarrow \mathcal{T}(\boldsymbol{m}) = (m_x, -m_y, m_z). \quad (6)$$

This means that the states that break the time-reversal symmetry must have $m_y \neq 0$. This is, for example, enforced by $\beta_{xx}^{\boldsymbol{m}} > 0$, since it penalizes m_x^2. The other details of the analysis of the potential can be found in the Supplemental Material [16]. The essential features can be qualitatively summarized as follows: First, all of the coefficients involving a y index vanish: $\alpha_y^{\boldsymbol{m}} = \beta_{ay}^{\boldsymbol{m}} = \beta_{ya}^{\boldsymbol{m}} = 0$. Moreover, the criterion for the condensation is $\alpha_0^{\boldsymbol{m}2} < \alpha_x^{\boldsymbol{m}2} + \alpha_z^{\boldsymbol{m}2}$, and also $\beta_{00}^{\boldsymbol{m}}, \beta_{zz}^{\boldsymbol{m}} > 0$.

The quadrupling phase appears when the mean-field approximation for the pairing fields is relaxed. The model (5) can be viewed as a mean-field approximation for the fermion quadrupling fields in a resistive state, such as the $\mathbb{Z}_2$-metal reported in [1]. Since superconducting currents are absent in the resistive state, the magnetic field caused by the gradients in the fermion quadrupling fields becomes

$$\boldsymbol{B} = -\frac{\epsilon_{abc} m_a \boldsymbol{\nabla} m_b \times \boldsymbol{\nabla} m_c}{4e\|\boldsymbol{m}\|^3}. \quad (7)$$

In two spatial dimensions, the topological invariant, which is associated with the degree of the maps $\boldsymbol{m}/\|m\|: \mathbb{S}^2 \mapsto \mathbb{S}^2_{\boldsymbol{m}}$, reads as

$$\mathcal{Q}(\boldsymbol{m}) = \frac{1}{4\pi}\int_{\mathbb{R}^2} \frac{\boldsymbol{m}\cdot\partial_x\boldsymbol{m}\times\partial_y\boldsymbol{m}}{\|\boldsymbol{m}\|^3} dxdy. \quad (8)$$

The integrand is obviously ill defined when $\|\boldsymbol{m}\| = 0$. However, whenever $\|\boldsymbol{m}\| \neq 0$, the corresponding configuration has an integer topological charge $\mathcal{Q}(\boldsymbol{m}) \in \mathbb{Z}$; this suggests that the model can host skyrmion topological excitations. Note that in three dimensions the model is characterized by another invariant, the Hopf invariant, which is associated with the maps $\mathbb{S}^3 \mapsto \mathbb{S}^2_{\boldsymbol{m}}$. This suggests the existence of hopfions, but it is beyond the scope of the current discussion.

The model describing the resistive fermion quadrupling state is like the Faddeev-Skyrme model [47]. This suggests that it could host nontrivial topological excitation such as skyrmions and hopfions. To investigate the properties of the topological defects of the effective model, the physical degrees of freedom $\boldsymbol{m}$ are discretized within a finite-element formulation [48], and the free energy (5) is minimized using a nonlinear conjugate gradient algorithm. For details of the numerical procedure, see [16].

The experiments [1] reported spontaneous magnetic fields in the quartic metal state. In the $s + is$ superconducting state, spontaneous magnetic fields can arise due to inhomogeneities such as thermal gradients [1,49], a hot spot created by a laser pulse [38], the effect of impurities [50,51], and other inhomogeneous arrays [4,40]. The material has slight inhomogeneity in doping level, which results in relatively small local modulation of the superconducting critical temperature [52]. Since for this topic the relative values of the gaps and phases strongly depend on doping, this can be modeled by spatial modulation of the prefactors of the quadratic terms of the Ginzburg-Landau theory. Implementing smoothly spatially varying amplitudes of the individual components, at the level of the effective model, can thus be modeled by small spatial variations of the coupling constants $\alpha_0^{\boldsymbol{m}}$ and $\alpha_z^{\boldsymbol{m}}$ (see Supplemental Material for details [16]). As shown in Fig. 1, such inhomogeneities in the effective model for the fermion quadrupling state, which break the time-reversal symmetry, result in spontaneous magnetic fields. It is qualitatively in accordance with the experiment [1].

First note that because the time-reversal symmetry ($\mathbb{Z}_2$) is broken, the model has domain-wall excitations. These are similar, in a way, to the domain walls found in a three-component model [1,53]. They are thus discussed in the Supplemental Material [16]. However the quantization of $\mathcal{Q}(\boldsymbol{m})$ suggests that the model has more nontrivial topological excitations with quantized magnetic flux according to $\int B_z = \Phi_0\mathcal{Q}$, where $\Phi_0 = -2\pi/e$ is the flux quantum. If a model breaks the $\mathbb{Z}_2$ symmetry and has only gradient terms which are second order in derivatives, according to the Hobart-Derrick theorem [54,55], skyrmions cannot exist. In our case, the presence of the Skyrme term, in the effective model (5), allows for nontrivial configurations that evade the Hobart-Derrick theorem. Indeed, in two dimensions, the Skyrme term in the effective model scales as $1/R^2$ (where R is a texture size), and therefore stable

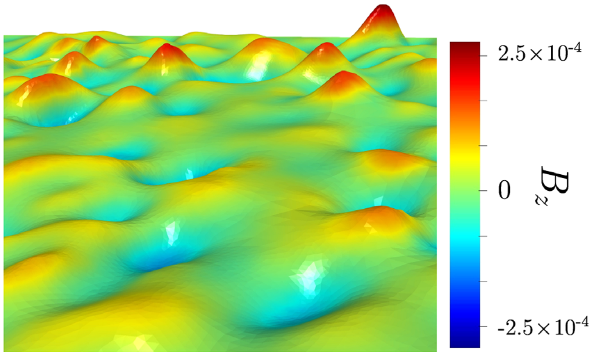

FIG. 1. Spontaneous magnetic field $\boldsymbol{B}$ (7) in the quartic phase, generated by inhomogeneities. The inhomogeneities are modeled by random spatial modulation of the parameters $\alpha_0^{\boldsymbol{m}}$ and $\alpha_z^{\boldsymbol{m}}$, reflecting the naturally present weak gradients in doping level. The surface elevation, together with the coloring, represents the magnitude of the B_z. The coupling here is $e = 0.6$, and the other parameters are given in the Supplemental Material [16].

skyrmions may exist due to the competition between the Skyrme and potential terms.

We performed numerical simulation by minimizing the energy (5) from various initial states. When the initial guess has a nontrivial topological charge, the minimization procedure leads, after convergence of the algorithm, to stable skyrmion configurations. Figure 2 shows these skyrmions solutions for increasing values of the topological charge $\mathcal{Q}(\boldsymbol{m})$, which is integer with an accuracy around 10^{-4}. As shown on the middle row of Fig. 2, the skyrmions carry a nonzero magnetic field. Moreover, since the topological charge (8) is quantized, the skyrmions carry integer quanta of magnetic flux. The circulating current pattern that induces this magnetic field is illustrated in the bottom row. This current, defined according to Ampère's law for the magnetic field (7) corresponds to the charge-carrying counterflow between the different components.

Furthermore we find that the interskyrmion forces are attractive. Hence, single quanta skyrmions attract each other to form skyrmions with higher topological charge. Thus in general one would not expect the formation of regular skyrmion lattices but rather skyrmion lumps formed by the competition between the attractive forces and pinning landscape. Interestingly, in a single quantum skyrmion, the time-reversed state is realized at a zero measure area inside the skyrmion. On the other hand, skyrmions carrying more than one quantum feature inner regions of the time-reversed state. The enclosed area of the time-reversed state increases with the topological charge. This suggests that if the $\mathbb{Z}_2$ symmetry associated with the relative phase locking is strongly broken, the formation of skyrmions is strongly inhibited. Note that unlike in Fig. 1, the parameters for the skyrmions displayed in Fig. 2 are homogeneous, as we focus here on the detailed structure of the skyrmions. Inhomogeneities can however deform the skyrmions, although we find that they do not destroy skyrmions (see Supplemental Material for details [16]).

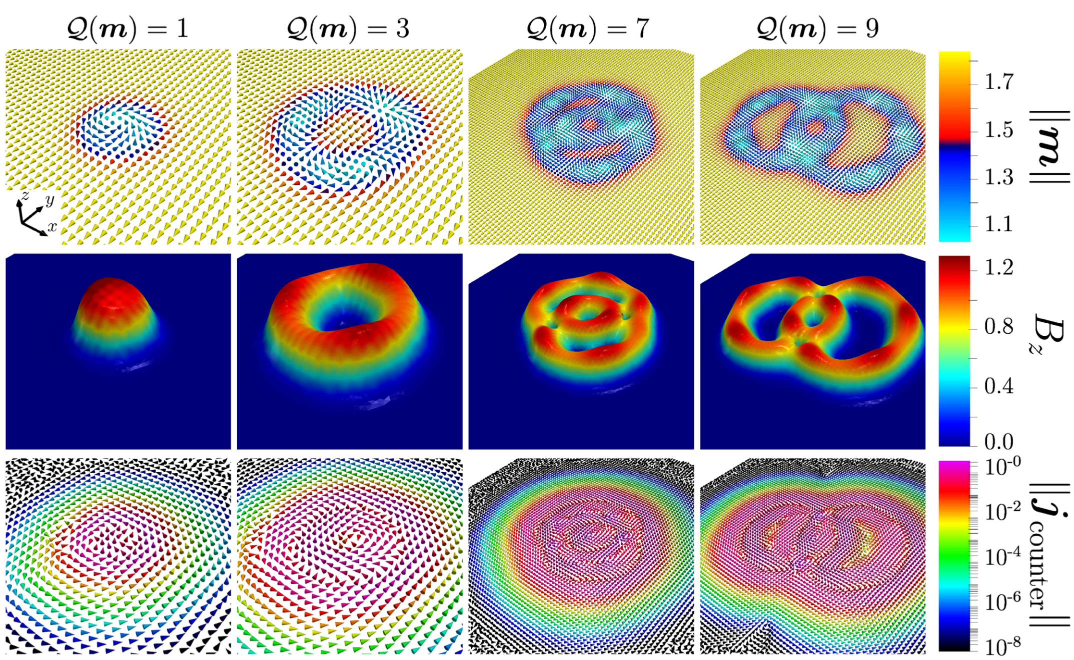

FIG. 2. Skyrmion solutions in a time-reversal symmetry broken state, for increasing values of the topological charge $\mathcal{Q}(\boldsymbol{m})$. The panels on the top row display the texture of the four-fermion order parameter $\boldsymbol{m}$. The panels in the middle row show the associated magnetic field $\boldsymbol{B}$ (7), and the bottom row shows the corresponding charge transferring counter-currents $\boldsymbol{j}_{\text{counter}}$ according to Ampère's law. The parameters are the same as in Fig. 1, while the coupling $e = 0.25$.

The recent experiment reported a fermion quadrupling phase in $Ba_{1-x}K_xFe_2As_2$ [1]. In this resistive phase, there is no condensate of Cooper pairs, but a four-fermion condensate which breaks the $\mathbb{Z}_2$ time-reversal symmetry.

We derived an effective model of that resistive state, starting from a microscopic three-band model with dominant interband interaction for $Ba_{1-x}K_xFe_2As_2$ and by implementing a mean-field approximation for the fields that are fourth order in fermions. The effective field theory has a structure similar to the Faddeev-Skyrme model, but for a soft modulus vector field that represents the fermion quadrupling order parameter. If spatial inhomogeneities are present the model accounts for spontaneous magnetic fields, consistently with the experimental observations [1]. We report that despite the lack of Meissner effect and the lack of conserved U(1) topological charge, the model has stable topological excitations in the form of skyrmions with conserved topological charge given by (8).

We would like to remind the reader that, similarly to skyrmions that appear in other contexts, such as magnetism, their existence also depends on factors that are beyond the effective long-wavelength field-theoretic model. Namely, in contrast to vortices, the skyrmionic topological charge is obtained through a surface integral. Consequently, if the terms that break the O(3) symmetry are very strong, the localization of the skyrmionic topological charge can shrink down to scales where the effective theory is ill defined, thereby destroying the topological protection. When the effective field theory is applicable, the potential barrier preventing the collapse of a skyrmion in a film can be roughly estimated as follows: the condensation energy density (F_c) multiplied by the coherence volume $F_c\xi^2_{\mathbb{Z}_2}L$, where $\xi_{\mathbb{Z}_2}$ is the coherence length associated with the broken time-reversal symmetry and L is the film thickness.

Finally, within the range of applicability of the effective theory, the skyrmions can be induced by taking advantage of the Kibble-Zurek mechanism [56,57], by quenching the material through the $\mathbb{Z}_2$ phase transition where the time-reversal symmetry is broken. We expect that skyrmions may also form by cooling through the phase transition with an applied *local* magnetic field induced through a system of coils.

We thank Vadim Grinenko for discussions. The computations were performed on resources provided by the Swedish National Infrastructure for Computing (SNIC) at the National Supercomputer Center at Linköping, Sweden. The work was supported by the Swedish Research Council Grants No. 2016-06122 and No. 2018-03659.

*garaud.phys@gmail.com
†babaev.egor@gmail.com

[1] V. Grinenko, D. Weston, F. Caglieris, C. Wuttke, C. Hess, T. Gottschall, I. Maccari, D. Gorbunov, S. Zherlitsyn, J. Wosnitza, A. Rydh, K. Kihou, C.-H. Lee, R. Sarkar, S. Dengre, J. Garaud, A. Charnukha, R. Hühne, K. Nielsch, B. Büchner, H.-H. Klauss, and E. Babaev, State with spontaneously broken time-reversal symmetry above the superconducting phase transition, Nat. Phys. **17**, 1254 (2021).

[2] V. Grinenko, P. Materne, R. Sarkar, H. Luetkens, K. Kihou, C. H. Lee, S. Akhmadaliev, D. V. Efremov, S.-L. Drechsler, and H.-H. Klauss, Superconductivity with broken time-reversal symmetry in ion-irradiated $Ba_{0.27}K_{0.73}Fe_2As_2$ single crystals, Phys. Rev. B **95**, 214511 (2017).

[3] V. Grinenko, R. Sarkar, K. Kihou, C. H. Lee, I. Morozov, S. Aswartham, B. Büchner, P. Chekhonin, W. Skrotzki, K. Nenkov, R. Hühne, K. Nielsch, S. L. Drechsler, V. L. Vadimov, M. A. Silaev, P. A. Volkov, I. Eremin, H. Luetkens, and H.-H. Klauss, Superconductivity with broken time-reversal symmetry inside a superconducting s-wave state, Nat. Phys. **16**, 789 (2020).

[4] V. L. Vadimov and M. A. Silaev, Polarization of the spontaneous magnetic field and magnetic fluctuations in $s+is$ anisotropic multiband superconductors, Phys. Rev. B **98**, 104504 (2018).

[5] M. Speight, T. Winyard, A. Wormald, and E. Babaev, Magnetic field behavior in $s+is$ and $s+id$ superconductors: Twisting of applied and spontaneous fields, Phys. Rev. B **104**, 174515 (2021).

[6] V. Stanev and Z. Tešanović, Three-band superconductivity and the order parameter that breaks time-reversal symmetry, Phys. Rev. B **81**, 134522 (2010).

[7] J. Carlström, J. Garaud, and E. Babaev, Length scales, collective modes, and type-1.5 regimes in three-band superconductors, Phys. Rev. B **84**, 134518 (2011).

[8] S. Maiti and A. V. Chubukov, $s+is$ state with broken time-reversal symmetry in Fe-based superconductors, Phys. Rev. B **87**, 144511 (2013).

[9] M. Silaev, J. Garaud, and E. Babaev, Phase diagram of dirty two-band superconductors and observability of impurity-induced $s+is$ state, Phys. Rev. B **95**, 024517 (2017).

[10] J. Böker, P. A. Volkov, K. B. Efetov, and I. Eremin, $s+is$ superconductivity with incipient bands: Doping dependence and STM signatures, Phys. Rev. B **96**, 014517 (2017).

[11] E. Babaev, A. Sudbø, and N. W. Ashcroft, A superconductor to superfluid phase transition in liquid metallic hydrogen, Nature (London) **431**, 666 (2004).

[12] E. Babaev, Phase diagram of planar $\mathrm{U}(1)\times\mathrm{U}(1)$ superconductor Condensation of vortices with fractional flux and a superfluid state, arXiv:cond-mat/0201547v7.

[13] T. A. Bojesen, E. Babaev, and A. Sudbø, Time reversal symmetry breakdown in normal and superconducting states in frustrated three-band systems, Phys. Rev. B **88**, 220511 (R) (2013).

[14] T. A. Bojesen, E. Babaev, and A. Sudbø, Phase transitions and anomalous normal state in superconductors with broken time-reversal symmetry, Phys. Rev. B **89**, 104509 (2014).

[15] J. Carlström and E. Babaev, Spontaneous breakdown of time-reversal symmetry induced by thermal fluctuations, Phys. Rev. B **91**, 140504(R) (2015).

[16] See Supplemental Material at http://link.aps.org/supplemental/10.1103/PhysRevLett.129.087602, which includes Refs. [17–24], for detailed derivation, additional results, and discussion of the numerical methods.

[17] E. Babaev, Non-Meissner electrodynamics and knotted solitons in two-component superconductors, Phys. Rev. B **79**, 104506 (2009).

[18] J. Garaud, K. A. H. Sellin, J. Jäykkä, and E. Babaev, Skyrmions induced by dissipationless drag in $U(1) \times U(1)$ superconductors, Phys. Rev. B **89**, 104508 (2014).

[19] D. V. Hutton, *Fundamentals of Finite Element Analysis*, Engineering Series (McGraw-Hill, New York, 2003).

[20] J. Reddy, *An Introduction to the Finite Element Method* (McGraw-Hill Education, New York, 2005).

[21] R. Fletcher and C. M. Reeves, Function minimization by conjugate gradients, Computer Journal (UK) **7**, 149 (1964).

[22] E. Polak and G. Ribière, Note sur la convergence de directions conjuguées, Revue française d'informatique et de recherche opérationnelle (R.I.R.O.), Série rouge **3**, 35 (1969).

[23] B. T. Polyak, The conjugate gradient method in extremal problems, USSR Computational Mathematics and Mathematical Physics **9**, 94 (1969).

[24] J. R. Shewchuk, *An Introduction to the Conjugate Gradient Method without the Agonizing Pain*, Technical Report (Carnegie Mellon University, Pittsburgh, PA, USA, 1994).

[25] C.-W. Cho, J. Shen, J. Lyu, O. Atanov, Q. Chen, S. H. Lee, Y. S. Hor, D. J. Gawryluk, E. Pomjakushina, M. Bartkowiak, M. Hecker, J. Schmalian, and R. Lortz, Z_3-vestigial nematic order due to superconducting fluctuations in the doped topological insulators $NbxBi_2Se_3$ and $Cu_xBi_2Se_3$, Nat. Commun. **11**, 3056 (2020).

[26] A. B. Kuklov, M. Matsumoto, N. V. Prokof'ev, B. V. Svistunov, and M. Troyer, Deconfined Criticality: Generic First-Order Transition in the SU(2) Symmetry Case, Phys. Rev. Lett. **101**, 050405 (2008).

[27] E. V. Herland, Tr. A. Bojesen, E. Babaev, and A. Sudbø, Phase structure and phase transitions in a three-dimensional SU(2) superconductor, Phys. Rev. B **87**, 134503 (2013).

[28] D. F. Agterberg and H. Tsunetsugu, Dislocations and vortices in pair-density-wave superconductors, Nat. Phys. **4**, 639 (2008).

[29] E. Berg, E. Fradkin, and S. A. Kivelson, Charge-4e superconductivity from pair-density-wave order in certain high-temperature superconductors, Nat. Phys. **5**, 830 (2009).

[30] A. B. Kuklov, N. V. Proko'ev, B. V. Svistunov, and M. Troyer, Deconfined criticality, runaway flow in the two-component scalar electrodynamics and weak first-order superfluid-solid transitions, Ann. Phys. (Amsterdam) **321**, 1602 (2006), Special Issue.

[31] O. Erten, P.-Y. Chang, P. Coleman, and A. M. Tsvelik, Skyrme Insulators: Insulators at the Brink of Superconductivity, Phys. Rev. Lett. **119**, 057603 (2017).

[32] V. Fleurov and A. Kuklov, Cooperative phases and phase transitions of Bose condensed light in dye filled cavities, New J. Phys. **21**, 083009 (2019).

[33] D. Shaffer, J. Wang, and L. H. Santos, Theory of Hofstadter superconductors, Phys. Rev. B **104**, 184501 (2021).

[34] F. L. Buessen, S. Sorn, I. Martin, and A. Paramekanti, Nematic order driven by superconducting correlations, Ann. Phys. (Amsterdam) **435**, 168494 (2021).

[35] Rafael M. Fernandes and Liang Fu, Charge-4e Superconductivity from Multicomponent Nematic Pairing: Application to Twisted Bilayer Graphene, Phys. Rev. Lett. **127**, 047001 (2021).

[36] S. B. Chung and S. K. Kim, Berezinskii-Kosterlitz-Thouless transition transport in spin-triplet superconductor, SciPost Physics Core **5**, 003 (2022).

[37] V. Drouin-Touchette, P. P. Orth, P. Coleman, P. Chandra, and T. C. Lubensky, Emergent Potts Order in a Coupled Hexatic-Nematic XY model, Phys. Rev. X **12**, 011043 (2022).

[38] J. Garaud, M. Silaev, and E. Babaev, Thermoelectric Signatures of Time-Reversal Symmetry Breaking States in Multiband Superconductors, Phys. Rev. Lett. **116**, 097002 (2016).

[39] J. Garaud, M. Silaev, and E. Babaev, Microscopically derived multi-component Ginzburg–Landau theories for $s + is$ superconducting state, Physica (Amsterdam) **533C**, 63 (2017).

[40] J. Garaud, A. Corticelli, M. Silaev, and E. Babaev, Properties of dirty two-band superconductors with repulsive interband interaction: Normal modes, length scales, vortices, and magnetic response, Phys. Rev. B **98**, 014520 (2018).

[41] E. Babaev, L. D. Faddeev, and A. J. Niemi, Hidden symmetry and knot solitons in a charged two-condensate Bose system, Phys. Rev. B **65**, 100512(R) (2002).

[42] J. Garaud, J. Carlström, E. Babaev, and M. Speight, Chiral $\mathbb{C}P^2$ skyrmions in three-band superconductors, Phys. Rev. B **87**, 014507 (2013).

[43] E. Smørgrav, E. Babaev, J. Smiseth, and A. Sudbø, Observation of a Metallic Superfluid in a Numerical Experiment, Phys. Rev. Lett. **95**, 135301 (2005).

[44] J. Smiseth, E. Smørgrav, E. Babaev, and A. Sudbø, Field- and temperature-induced topological phase transitions in the three-dimensional N-component London superconductor, Phys. Rev. B **71**, 214509 (2005).

[45] D. Weston and E. Babaev, Composite order in SU(N) theories coupled to an Abelian gauge field, Phys. Rev. B **104**, 075116 (2021).

[46] This is because the topological charge of composite, single-quantum superconducting vortex has a winding only in the phase sum. Hence it cannot restore order in the fields that depend only on the relative phases and relative densities.

[47] L. D. Faddeev and A. J. Niemi, Knots and particles, Nature (London) **387**, 58 (1997).

[48] F. Hecht, New development in freefem++, J. Numer. Math. **20**, 251 (2012); See also FreeFEM software at https://freefem.org/.

[49] M. Silaev, J. Garaud, and E. Babaev, Unconventional thermoelectric effect in superconductors that break time-reversal symmetry, Phys. Rev. B **92**, 174510 (2015).

[50] S. Maiti, M. Sigrist, and A. Chubukov, Spontaneous currents in a superconductor with $s + is$ symmetry, Phys. Rev. B **91**, 161102(R) (2015).

[51] S.-Z. Lin, S. Maiti, and A. Chubukov, Distinguishing between $s + id$ and $s + is$ pairing symmetries in multiband superconductors through spontaneous magnetization

pattern induced by a defect, Phys. Rev. B **94**, 064519 (2016).

[52] Y. Iguchi *et al.* (to be published).

[53] J. Garaud and E. Babaev, Domain Walls and Their Experimental Signatures in $s + is$ Superconductors, Phys. Rev. Lett. **112**, 017003 (2014).

[54] R. H. Hobart, On the instability of a class of unitary field models, Proc. Phys. Soc. **82**, 201 (1963).

[55] G. H. Derrick, Comments on nonlinear wave equations as models for elementary particles, J. Math. Phys. (N.Y.) **5**, 1252 (1964).

[56] T. W. B. Kibble, Topology of cosmic domains and strings, J. Phys. A **9**, 1387 (1976).

[57] W. H. Zurek, Cosmological experiments in superfluid helium?, Nature (London) **317**, 505 (1985).